

Short Thesis for the Degree of Doctor of Philosophy (PhD)

**Investigation of image quality optimization methods for
Positron Emission Tomography in hybrid medical imaging**

Áron Krisztián Krizsán
Supervisor: László Balkay, PhD



UNIVERSITY OF DEBRECEN

DOCTORAL SCHOOL OF MOLECULAR MEDICINE

Debrecen, 2016

Investigation of image quality optimization methods for Positron Emission Tomography in hybrid medical imaging

Written by Áron Krisztián Krizsán, MSc

Supervisor: László Balkay, PhD

Doctoral School of Molecular Medicine, University of Debrecen

Head of the **Examination Committee**:

László Csernoch, PhD, DSc

Members of the Examination Committee:

Zsolt Bacsó, MD, PhD

Krisztián Szigeti, PhD

The Examination takes place at the library of the Department of Physiology, Faculty of Medicine, University of Debrecen at 12:00 am, 26th of April, 2016.

Head of the Defense Committee:

László Csernoch, PhD, DSc

Reviewers:

Martin Paul Tornai, PhD

Dávid Légrády, PhD

Members of the Defense Committee:

Zsolt Bacsó, MD, PhD

Krisztián Szigeti, PhD

The PhD Defense takes place at the Lecture Hall of Bldg. A, Department of Internal Medicine, Faculty of Medicine, University of Debrecen at 14:00, 26th of April, 2016.

1. Introduction

Positron Emission Tomography (PET) is a non-invasive functional imaging method that has become widely used in the nuclear medicine field during the last three decades. PET incorporates the unique characteristics of radionuclides decay with positron emission. Such radionuclides are usually produced in a cyclotron and then used to label a medically interested molecule for the purpose of tracing its metabolism processes. Radiotracers commonly used in PET for example are the followings: ^{18}F -FDG may indicate normal or pathological glucose uptake in the gray matter or could show increased glucose metabolism in tumor tissue, ^{18}F -Fallypride accumulation in the brain could reveal dopamine D2 receptors in the striatum, ^{11}C -PiB could show specific or non-specific binding to amyloid- β , and therefore give information on pathology in case of Alzheimer disease. Furthermore, an important characteristic of PET is the quantitative aspect of the method. If the scanner is correctly calibrated and all necessary corrections on the raw data are performed (Detector normalization, Attenuation-, Scatter- and Random corrections), the image pixel or voxel intensities (counts per second in a voxel) could be converted to activity concentration units (kBq/ml). This information is then used to detect pathological uptakes and plan on the appropriate therapy. All of these characteristics fostered the capabilities of PET to be one of the leading functional imaging techniques in medical diagnostics. Both anatomical and functional imaging methods had many developments in the last two decades, while the greatest advancement of PET was probably the introduction of this method in hybrid imaging, first with PET/CT and then with PET/MRI.

Among other performance parameters, image noise, especially in terms of Signal to Noise Ratio (SNR) plays a very important role in describing the quality of medical images. For measuring and describing noise, several methods could be used based on the focus of the study and the depth of information needed. The noise of medical images is called in several contexts as image uniformity, or background variability and even SNR or Contrast to noise Ratio (CNR). The SNR is depending on the detector technology, including the detection efficiency and the readout logic of the scintillator crystals. Among the new hybrid technologies, the introduction of PET/MRI had great attention in the medical imaging field worldwide. The inclusion of both modalities in a single device demanded solutions of complex engineering challenges, especially in terms of PET detectors to operate in high magnetic fields. Conventional PMT detectors benefit from high signal gain in the range of 10^5 - 10^7 . Low noise and fast transit time (~ 100 ps) are also available today, and have made this photo-sensor the first candidate for application involving the TOF PET technology. However, in strong magnetic field PMT technology is not able to produce acceptable position maps for imaging purposes. New photo-detector concepts using semi-conductors called Avalanche Photodiodes (APDs) provided a solution for this problem and have been already used efficiently for PET when near strong magnets. However the SNR performance of these applications is lower compared to former PET technology because APDs have significantly higher rise times (up to 2-3 ns) that prevent adequate timing resolution for TOF. Furthermore the low gain ($\sim 10^2$) remained a disadvantage of APDs as well. Coupling LSO crystals with newly

introduced Silicon Photo-Multiplier (SiPM) technology resulted in timing resolution sufficient for TOF measurements. The considerably lower noise of SiPMs (compared to the APDs) and high gain ($\sim 10^6$) are the additional promising features of SiPM, which made this technology suitable for PET photo-detectors for advanced PET/MRI systems. It needs to be noted that PMTs have lower noise characteristics compared to APDs or SiPMs. Some approaches for the inclusion of SiPM in a full-ring PET detector system have already been introduced successfully. These developments were mainly focusing on preclinical PET imaging devices, however the human applications are already in the production phase and will be available in the near future. While many research groups reported on good results of SiPM PET applications, our institutions also started to work on the direct comparison of SiPM with conventional PMT technology on PET scanner performance and imaging capabilities. We developed two preclinical imaging systems: the MiniPET-2 with PMT technology and the MiniPET-3 using SiPM detectors. The geometrical parameters, the scintillation crystal material, data acquisition system, image reconstruction methods of the two cameras were kept the same. Another great advantage of SiPMs is the possible one-to-one coupling with scintillation crystals that could eliminate the position map coding error of the conventional analog PMT method, and therefore contribute to better spatial resolution. This has an impact even on the time resolution of the scanner and therefore gives an improvement compared to former TOF gained SNR with a factor of two. These advancements apply for both PET/CT and PET/MRI techniques

and therefore are very promising in case of recently introduced and future hybrid systems.

Besides using appropriate detector technology in hybrid imaging, it is important to optimize the scanning protocols and the reconstruction methods for both patient characteristics and scanner properties. In the clinical PET/CT protocols the acquisition time necessary to collect enough counts to produce images of high diagnostic quality depends on several factors, including scanner sensitivity, imaging mode (2-D or 3-D) and patient weight. Both, the number of total counts acquired during the acquisition and the quality of PET images are negatively correlated with the weight of the patient. Extended acquisition times are typically required for heavier patients (rather than increasing administered dose) in order to maintain image quality. Image data for PET studies are typically collected in discrete axial bed positions in most cases. The acquisition scan duration is usually adjusted according to the weight or the Body Mass Index (BMI) of the patient. Although the total acquisition time is adjusted to the patient body properties, the acquisition time at each bed position is kept constant. This means that a body section where there is less attenuation (head and neck) will have the same acquisition time as a section where there is more significant attenuation (abdomen). As the different sections of the body have various gamma photon attenuation factors and activity distribution as well, it is expected that the image SNR will vary accordingly. During the clinical reading process of the images the constant SNR would be preferable, therefore methods to optimize acquisition durations of bed positions would be necessary for the harmonization of SNR axially. This concept of varying

the acquisition time durations of different bed positions may be seen as be analogous to the Tube Current Modulation (also known as Automatic Exposure Control) used in X-ray CT for dose reduction; however, in PET the time modulation could be used to equalize image SNR axially.

2. Aims

While the importance of SiPM technology in hybrid systems (such as PET/CT and PET/MRI) is significant, we had a unique setting of two preclinical PET scanners for direct comparison with the conventional technology. The MiniPET-2 includes PMT photosensors and the MiniPET-3 has SiPMs but the geometrical parameters, the scintillation crystal material, data acquisition system, image reconstruction methods of the two cameras were kept the same. We aimed to:

1. Perform a direct comparison by measurements as specified by the NEMA NU 4-2008 standard protocols, extended with energy resolution and coincidence time window optimization measurements.
2. Report on the first complete performance and imaging capability evaluation of a SiPM based preclinical PET scanner using this NEMA standard.
3. Evaluate the imaging and performance data with the same software environment.
4. Perform computer simulations to describe the characteristics of a human scale scanner based on the MiniPET concepts.

In addition, we started to work on the optimization of patient scanning protocols of human Whole Body PET scans to harmonize image noise axially. While many approaches are available to determine SNR for human whole body PET imaging, we used pixel-wise the Standard Deviation/Mean (SD/Mean) values on series of image sets,

hence this measure gives the appropriate depth of information for this study. We aimed to:

1. Investigate the possibility of varying the acquisition time for different sections of the body such that the image SNR is kept relatively constant for all slices.
2. To estimate the acquisition times for the different sections of the body we propose to use the sinogram of attenuation correction factors (ACFs) generated from the CT scan that is typically acquired prior to the PET scan.
3. Perform both computer simulations (based on real CT patient data) and evaluations of phantom and patient PET measurement data for the proof of this new concept.

3. Materials and Methods

3. 1. NEMA NU 4 Comparison of the PMT based MiniPET-2 and the SiPM based MiniPET-3 scanners.

The significant difference between the two MiniPET systems lies in the photo-sensors: the MiniPET-2 includes conventional PMTs, while the MiniPET-3 uses SiPMs and a readout system optimized for this type of detectors. A row – column readout of the SiPM matrix was used without applying individual signal processing channels to each matrix element. Weighting circuits were connected directly to the row– and column– outputs as proposed by Y. Wang et al., but modified in such a way as to reduce the dark noise. Data from the detector modules were transmitted to the data acquisition computer via the 100BASE-TX Ethernet network system. The custom made MultiModal Medical Imaging (M3I) software library was developed for the tasks of data collection and processing such as primary data processing, scanner calibration, image reconstruction, image processing and evaluation of performance parameters. This software tool arranges the data into 3D Line Of Response (LOR) or single events list-mode data files that can be histogrammed into 2D sinograms. The M3I performs 2D Maximum Likelihood Expectation Maximization (ML-EM) that we used in case of the image quality measurements. All necessary measurements proposed in the NEMA NU 4–2008 standard were performed on both MiniPET systems including: spatial resolution, system sensitivity, image quality

(recovery coefficients of 5 different diameter rods, uniformity of a uniform cylinder phantom region, spill over ratios in water and air chambers of the phantom) and count rate performance measurements. In addition, coincidence time window optimization, energy resolution and position map evaluations were also performed. Besides the MiniPET comparison measurements and evaluations, we designed simulations to estimate the performance of a human brain PET scanner based on the MiniPET detector concepts. For the simulations we used the GATE software package and the Hyper Performance Computing machines of the University of Debrecen.

3. 2. Whole body PET image SNR optimization using variable acquisition times

Computer simulations were performed to estimate the effect of varied acquisition time aiming equalized SNR characteristics axially. To estimate the effect of attenuation on image SNR a series of simulations was performed based on whole body CT scans. From the CT scans, attenuation correction factors were generated using the standard bi-linear scaling method. Taking the same CT images, a uniform activity distribution in soft tissue was generated. To estimate the noise distribution in the images, Poisson noise was added to the backprojected images (sinograms), and 20 noise replicates were generated. Each replicate was corrected for attenuation and reconstructed using iterative image reconstruction. From the 20 replicates, pixel-wise Mean and SD images were generated. For each axial body slice a region of interest

(ROI) analysis was performed. The correlation between the SD/Mean values and the average attenuation correction factors (averaged over all angles) passing through the center of the body was also investigated. In addition to the patient outline shaped cylinder, circular and elliptical simulations were performed similarly as the patient simulations. To estimate the relative acquisition times along the axial direction of the body, a circular ROI analysis was applied on each of the reconstructed emission Mean and SD images. For each slice the square of the SD divided by the Mean was calculated from the average pixel intensities of the defined ROI on both image sets. Using the slice with the average $(SD/Mean)^2$ value (among all slices) as a reference, the relative acquisition time that would yield a uniform SD/Mean for all slices was calculated as:

$$T_i = \frac{T_{total}}{n} \times \frac{(SD / Mean)_i^2}{(SD / Mean)_{ref}^2}$$

where i means the slice number, T_{total} the total scan time and n the number of axial scan positions. Based on the results from the simulations, a PET scan with a set of different diameter phantoms was acquired on a Siemens Biograph 64 Truepoint PET/CT system. Three cylinders with different diameters, a NEMA image quality phantom with no activity in the spheres or in the lung insert, and an Anthropomorphic Phantom were filled with ^{18}F -Fluoro-Deoxy-Glucose. A list mode dataset was acquired of each phantom from which 20 bootstrap replicates (fixed and variable times) were generated. For SNR estimation

we used the so-called bootstrap method. Each bootstrap replicate was reconstructed using iterative reconstruction. Mean and SD images were generated pixel-by-pixel from the set of replicate images. An ROI analysis was performed for both the Mean and SD images and central average AC factors were also calculated from the CT derived attenuation correction. A patient scan was also acquired as prompts and randoms, from which a pseudo-list mode data set was generated. Using this data set, 20 bootstrap replicates (fix and variable times) were generated. Each replicate was reconstructed using iterative OSEM method from which Mean and SD images were generated.

4. Results

4. 1. NEMA NU 4 Comparison of the PMT based MiniPET-2 and the SiPM based MiniPET-3 scanners.

In the performance comparison of the MiniPET systems we found similar imaging capabilities. According to the position maps: The average top/valley (T/V) ratios for the MiniPET-2 and MiniPET-3 detector modules are 5.20 ± 0.21 and 5.73 ± 1.03 , respectively. The highest T/V of the MiniPET-3 is more pronounced if we consider only the crystals in the high light collection position. In this case the average T/V is 6.6 ± 0.43 . The system average energy resolution values were measured to be 19.98 ± 7.59 % and 31.74 ± 11.30 % for the MiniPET -2 and MiniPET-3 respectively. Spatial resolution was approximately 17% better on average for the MiniPET-3 than the MiniPET-2. The axial system sensitivity was very similar for both scanners and both systems performed similarly in terms of peak absolute sensitivity ($\sim 1.37\%$)

According to the image quality phantom study, the smallest rod was more visible on the images acquired with the MiniPET-3 compared to that of the MiniPET-2. The SOR values found to be similar for both systems (~ 0.15 for SOR air and ~ 0.25 for SOR water), while the uniformity was 5.59% in the case of MiniPET-2 and 6.49% in case of MiniPET-3. RC values showed comparable results ($\sim 0.33, 0.59, 0.81, 0.89, \text{ and } 0.94$) for both of the MiniPET systems, while four rods showed slightly higher values in case of the MiniPET-3. Although, we observed that the total count rate performances have a maximum around

50 MBq activity level for both scanners, the peak NEC count was approximately twice as high for the MiniPET-3 than for the MiniPET-2 (14 kcps vs. 24 kcps) when using the larger phantom geometry. The optimal coincidence time window was 6 ns for the MiniPET-2 and 8 ns for the MiniPET-3.

In case of the human brain PET scanner simulation the position map peak/valley ratios were between five and ten, which is close to the MiniPET-3 corresponding values. The average energy resolution of the system is $26 \pm 12\%$, which is less than the measured value. NEC peak values were 37 kcps (at 135 MBq) and 150 kcps (at 38 MBq) for a smaller field of view (FOV) simulation and a larger FOV simulation respectively. The central system sensitivity was $\sim 14\%$, which is definitely higher than the MiniPET-3 corresponding value, and very close to the theoretical 17.9%.

4. 2. Whole body PET image SNR optimization using variable acquisition times

During the evaluation of the different cylinder simulations definite correlation was recognized between image SNR and the average AC factors regardless to the shape of the activity distribution. The patient simulations revealed that subjects with different weights (54.5-108.4 kg) showed the similar correlation between SNR and ACFs. The image SNR without and with equalization was investigated for a CT scan based simulation of a 73 kg patient. When no equalization was applied the noise level was the lowest in the head and neck region and as expected

the highest in the abdomen, where the attenuation is higher. Using the time adjustment equation and the correlation of the SNR and ACFs, the relative acquisition time (in form of the applied activity level on the image pixels) was adjusted. The relatively flat noise pattern indicated that this correlation can be used to adjust the acquisition time to equalize the image noise axially, in this simplified case. For the phantom measurements, $(SD/Mean)^2$ at different positions within each phantom (derived from ROI analysis) showed correlation with the AC factors generated from CT images of the scanner. The data were fit to a 2nd degree polynomial function. Using the time adjustment equation along with the measured correlation between $(SD/Mean)^2$ and the average ACFs, the acquisition times that would yield a uniform image noise were calculated. To generate shorter/longer scan times, a smaller/larger fraction of prompt- and random counts were used in each bootstrap replicate. The resulting image noise curve indicated equalized noise levels for the phantoms with different diameters. This was compared to the case when the acquisition times were kept constant, and therefore the SNR pattern was more heterogeneous. In case of the whole body FDG PET patient scan the resulting Mean, SD and $SD/Mean$ images were determined, while the acquisition time at each bed position was 120s. Moreover, the corresponding images where the acquisition time was adjusted according to the correlation between the Average ACF and $(SD/Mean)^2$ were also investigated. Although the Mean images do not show any appreciable difference, there are some visible differences in the $SD/Mean$ images. Along the central axis the noise appears to be slightly more uniform. The image noise in the abdomen is reduced due

to the longer acquisition time. Similarly, the image noise is higher in the lungs due to the shortened acquisition time in this region. Although varying the scan time did not produce an appreciable change in image quality for the patient study, the proposed technique may improve visualization of low activity lesions particularly in sections of the body with high absorption.

5. Summary

PET is a very target sensitive imaging method that is used worldwide both in clinical hybrid techniques (combined with CT or MRI) or preclinical applications. New semiconductor photo-detector technologies (i.e. SiPM) play an important role in hybrid imaging and the improvement of image SNR. A preclinical PET system, the MiniPET-3 uses state-of-the-art SiPM photosensors was constructed in our institutions. We compared the MiniPET-3 with the MiniPET-2, a system with the same crystal geometry but conventional PMTs. The standard measurements proposed by the NEMA NU 4 protocols were performed on both systems. In addition, this is the first complete NEMA study on a SiPM based preclinical PET scanner. Both scanners performed similarly in terms of system sensitivity, RC, SOR and SF. The system average energy resolution values were measured to be 19.98 ± 7.59 % and 31.74 ± 11.30 % for the MiniPET-2 and MiniPET-3 respectively. Main differences were found in image uniformity (5.59 for MiniPET-2 and 6.49 for MiniPET-3) and peak NEC values (14 kcps for MiniPET-2 and 24 kcps for MiniPET-3). The former is a result of the slightly better spatial resolution of the MiniPET-3 and the latter is the consequence of the significantly higher dead time factor of the MiniPET-2. Spatial resolution was approximately 17% better on average for the MiniPET-3 than the MiniPET-2. While overall the RC values showed similar performance, the smallest diameter rod was more visible on the images of the MiniPET-3, which is probably a result of the better spatial resolution. Based on these results we can conclude that the MRI-

compatible SiPM-based MiniPET-3 scanner shows comparable results with the conventional technology producing images of high quality for small animal imaging. In addition, we performed computer simulation of a human brain PET scanner using the MiniPET concept and determined position maps, energy resolution, system sensitivity and count rate performances. The results gave us an outlook for possible future human applications based on the MiniPET conclusions.

We investigated the possibility of varying the acquisition time at different sections of the body such that the image SNR was kept relatively constant for all slices. To estimate the acquisition times for the different sections of the body we proposed to use the AC sinogram generated from the CT scan that is acquired prior to the PET scan. Both simulations and phantom measurements of different diameter cylinders with activity distributions were performed. The image noise was estimated in every pixel from multiple replicate image sets. A simple polynomial function was found for both the simulations and the phantom measurement images to accurately describe the image noise as a function of AC factors. The findings of this work indicate that regional image SNR of human Whole Body PET scans can be made more uniform axially by adjusting the acquisition time per bed position according to the amount of attenuation. Instead of using a fixed scan time for each bed position, the acquisition can be extended in areas of high absorption and shortened in less absorbing sections of the body. The relative acquisition times can be quickly calculated using a simple functional relationship.

6. List of Publications



UNIVERSITY OF DEBRECEN
UNIVERSITY AND NATIONAL LIBRARY



Registry number: DEENK/259/2015.PL
Subject: Ph.D. List of Publications

Candidate: Áron Krisztián Krizsán
Neptun ID: JQQZBK
Doctoral School: Doctoral School of Molecular Medicine

List of publications related to the dissertation

- Krizsán, Á.K.**, Lajos, I., Dahlbom, M., Daver, F., Emri, M., Kis, S.A., Opposits, G., Pohubi, L., Pótári, N., Hegyesi, G., Kalinka, G., Gál, J., Imrek, J., Nagy, F., Valastyán, I., Király, B., Molnár, J., Sanfilippo, D., Balkay, L.: A Promising Future: Comparable Imaging Capability of MRI-Compatible Silicon Photomultiplier and Conventional Photosensor Preclinical PET Systems.
J. Nucl. Med. 56 (12), 1948-1953, 2015.
DOI: <http://dx.doi.org/10.2967/jnumed.115.157677>
IF:6.16 (2014)
- Krizsán, Á.K.**, Czernin, J., Balkay, L., Dahlbom, M.: Whole Body PET Imaging Using Variable Acquisition Times.
IEEE Trans. Nucl. Sci. 61 (1), 115-120, 2014.
DOI: <http://dx.doi.org/10.1109/NSSMIC.2011.6153747>
IF:1.283





List of other publications

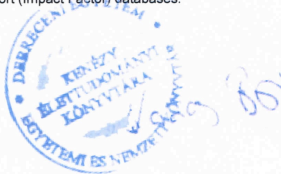
3. Balkay L., Emri M., **Krizsán Á.K.**, Opposits G., Varga J.: Újdonságok és új lehetőségek a funkcionális képkalkotásban: Leképezéstechnikai újdonságok.
Magyar Onkol. 59 (1), 4-9, 2015.
4. **Krizsán, Á.K.**, Varga, J., Forgács, A., Balkay, L.: Orvosi képkalkotás: Diagnosztika a képelemek mögött.
Fizikai Szle. 65 (3), 88-91, 2015.
5. Lajtos, I., Czernin, J., Dahlbom, M., Daver, F., Emri, M., Farshchi-Heydari, S., Forgács, A., Hoh, C.K., Józszai, I., **Krizsán, Á.K.**, Lantos, J., Major, P., Molnár, J., Opposits, G., Trón, L., Vera, D.R., Balkay, L.: Cold wall effect eliminating method to determine the contrast recovery coefficient for small animal PET scanners using the NEMA NU-4 image quality phantom.
Phys. Med. Biol. 59 (11), 2727-2746, 2014.
DOI: <http://dx.doi.org/10.1088/0031-9155/59/11/2727>
IF: 2.761
6. Lajtos I., Emri M., Trón L., Kis S.A., Opposits G., Márián T., Trencsényi G., Mikecz P., Spisák T., **Krizsán Á.K.**: A debreceni kisállat PET program eredményei: A MiniPET-1, MiniPET-2 és a MiniPET-3 kamerák leképezési tulajdonságai.
IME. 12 (különszám), 33-38, 2013.

Total IF of journals (all publications): 10,204

Total IF of journals (publications related to the dissertation): 7,443

The Candidate's publication data submitted to the iDEa Tudóstér have been validated by DEENK on the basis of Web of Science, Scopus and Journal Citation Report (Impact Factor) databases.

11 December, 2015



7. Further publications and abstracts

2015

Nagy, G., **Krizsán, Á.K.**, Forgács, A., Szolik, M., Dahlbom, M., Balkay, L.: Image noise estimation using sub-reconstructions of clinical Whole Body PET/CT data. *Eur. J. Nucl. Med. Mol. Imaging* 42 (Suppl. 1), S372., 2015.

2014

Jonsson, H.P., Pap, L.D., Forgács, A., Nagy, V., Dahlbom, M., Opposits, G., **Krizsán, Á.K.**, Garai, I., Czernin, J., Balkay, L.: Validation of intensity based tumor heterogeneity parameters in human PET diagnostics (P077). *Eur. J. Nucl. Med. Mol. Imaging* 41 (S2), S380., 2014.

Krizsán, Á.K., Lajtos, I., Emri, M., Kis, S.A., Opposits, G., Hegyesi, G., Kalinka, G., Gál, J., Király, B., Imrek, J., Valastyán, I., Molnár, J., Sanfilippo, D., Dahlbom, M., Balkay, L.: Performance Comparison of SiPM and PMT Based Preclinical PET Systems with Same Detector Geometries (P004). *Eur. J. Nucl. Med. Mol. Imaging* 41 (S2), S360., 2014.

2013

Krizsán, Á.K., Forgács, A., Garai, I., Balkay, L.: Reliability study of the calculated textural parameters for heterogenic activity distribution in PET investigation using special designed phantom. *Eur. J. Nucl. Med. Mol. Imag* 40 (Suppl. 2), S407., 2013.

Balkay, L., Forgács, A., **Krizsán, Á.K.**, Lajtos, I., Lengyel, Z., Garai, I., Azeez, A.: Accreditation quality control performances of different PET scanners. *Nucl. Med. Rev. Cent. East. Eur* 16 (Suppl. A), A18., 2013.

Krizsán, Á.K., Szolik, M., Nagy, G., Dahlbom, M., Balkay, L.: Noise analysis of whole body FDG PET images. *Nucl. Med. Rev. Cent. East. Eur* 16 (Supl. A), A17-A18., 2013.

Spisák, T., Opposits, G., Kis, S.A., Lajtos, I., **Krizsán, Á.K.**, Pohubi, L., Balkay, L., Emri, M.: BrainMOD: 4-dimensional multimodal medical image analysis software. In: Electronic presentation online system : ECR Congress 2013 / [ed. ESR], European Society of Radiology, [S. l.], C-2586, 2013.

2012

Balkay, L., Oszlánszki, A., **Krizsán, Á.K.**: Comparison of patient doses at different CT scanners with same acquisition protocol. *IEEE* 2012 3644-3645., 2012.

Krizsán, Á.K., Kis, S.A., Gál, J., Hegyesi, G., Balkay, L.: Simulation studies with SiPM arrays and LYSO crystal matrix analyzing a new readout scheme. In: IEEE Nuclear Science Symposium and Medical Imaging Conference : 19th International Workshop on room-temperature semiconductor x-ray and gamma-ray detectors / [ed. Nuclear and Plasma Sciences Society], Nuclear and Plasma Sciences Society, [S. l.], 205, 2012.

2011

Krizsán, Á.K., Czernin, J., Dahlbom, M.: Whole Body PET using variable acquisition times. *IEEE Trans. Nucl. Sci* M-200 1., 2011.

2008

Krizsán, Á.K., Füredi, A., Véső, T., Zalatnai, A., Valastyán, I., Balkay, L., Molnár, J., Molnár, J.: Effect of a new organosilicon multidrug resistance modifier on the metabolism of human

pancreatic cancer xenografts: Positron emission tomography study (PO 255). In: ICACT : Abstract Book : 19th International Congress of Anticancer treatment / [ed. D. Khayat, G. N. Hortobagyi], [S. n.], [S. l.], 342-343, 2008.